Shear loading of FCC/BCC Cu/Nb nanolaminates studied by in situ X-ray micro-diffraction

Etienne Navarro, Thomas Cornelius, Henry Proudhon, Rahul Sahay, Ihor Radchenko, Stéphanie Escoubas, Pooi See Lee, Nagarajan Raghavan, Arief Budiman, Olivier Thomas

Shear loading of FCC/BCC Cu/Nb nanolaminates studied by *in situ* X-Ray micro-diffraction

Etienne Navarro[1], Thomas W. Cornelius[1], Henry Proudhon[2], Rahul Sahay[3], Ihor Radchenko[3], Stéphanie Escoubas[1], Pooi See Lee[4], Nagarajan Raghavan[5], Arief S. Budiman[3,6,7], Olivier Thomas[1*]

[1]*Aix-Marseille Univ., Université de Toulon, CNRS, IM2NP, Marseille, France*
[2]*PSL Univ, MAT Ctr Mat, MINES ParisTech, CNRS,UMR 7633, BP 87, F-91003 Evry, France*
[3]*Xtreme Materials Lab, Engineering Product Development, Singapore University of Technology and Design (SUTD), Singapore*
[4]*School of Materials Science and Engineering, Nanyang Technological University, Singapore*
[5]*nano-Micro Reliability Lab (MRL), Engineering Product Development, Singapore University of Technology and Design (SUTD), Singapore*
[6]*Department of Manufacturing and Mechanical Engineering and Technology, Oregon Institute of Technology, Klamath Falls, OR 97601, USA*
[7]Industrial Engineering Department, BINUS Graduate Program – Master of Industrial Engineering, Bina Nusantara University, Jakarta, 11480, Indonesia

Abstract

Face-centered cubic/body centered cubic (FCC/BCC) nanolaminates prepared by Accumulative Roll Bonding (ARB) have been extensively studied because of their unique mechanical properties. Recently, micro-beam bending experiments, performed on Cu/Nb ARB samples, have shown an anisotropic interface sliding behavior linked to the strong in-plane texture. To test interface sliding on a macroscale we have developed a shear test based upon a specific sample geometry and on *in situ* tensile loading on an X-ray synchrotron beamline. As received nanolaminate samples exhibit a very anisotropic crystallographic texture as expected from the fabrication process. *In situ* X-ray diffraction in the sheared zone during mechanical loading yields strains in Cu and Nb. Early brittle failure prevents investigating further the sliding at interfaces. This is probably caused by crack initiation from the inner surfaces of the notches used to induce shear.

Introduction

FCC/BCC nanolaminates prepared by Accumulative Roll Bonding (ARB) have been extensively studied because of their unique mechanical properties. They offer a unique combination of strength (~1 GPa) and ductility (~ 10%) [1]. The origin of these properties is still under debate but the resistance of interfaces to dislocation motion is identified as a key factor triggered by parameters such as the misfit stress between alternating metal layers, their crystallographic misorientation, the ability of the interface to shear… Metallic FCC/BCC nanolayers, such as Cu/Nb, have also been shown to exhibit significant and tunable interfacial sliding (based on defect structures in the interface) [2,3]. This sliding at solid-solid interfaces raises many fundamental questions [4-6]. In previous works [2,3] sliding has been evidenced through three-point bending of microbeams and has been shown to be strongly anisotropic with sliding occurring along the Transverse Direction (TD) but not along the Rolling Direction (RD). This anisotropic shear strength is confirmed by Molecular Dynamics simulations [7] as well as experiments [8,9]. The microbeam bending experiments [2, 3] were performed on a scale comparable to the grain size and one may wonder whether the sliding would occur on a macroscopic scale or whether grain boundaries would impede sliding. This bears important consequences for applications since the existence of significant interfacial sliding all along on a macroscopic scale while maintaining full contact between the layers would lead to negligible electrical resistance increase upon straining. This would be attractive for stretchable metallic conductor technology.

Atomic reconfigurations associated with interface-based deformation have enabled recent scientific discoveries, involving the findings of extraordinary mechanical properties [10-13] and radiation-damage tolerance [14,15] in Cu/Nb nanolayers making them withstand extreme environments (strain, strain rate/shock extremes [16,17], self-healing [18, 19] and radiation damage [14,19]). Beyond Cu/Nb nanolayered systems, the intriguing possibility of frictionless gliding of one solid surface on another has been predicted for certain incommensurate interfaces in crystals, based on Aubry's solution to the Frenkel-Kontorova model [4] of a harmonic chain in a periodic potential field. Incommensurate structures hold a special place in the science of crystalline materials and especially in the study of the exact roles of defects in influencing the overall response of the crystal upon mechanical deformation. Incommensurability arises when translational symmetries with different but incompatible repeat patterns interact, such as interfaces between two different crystals. Even single-phase materials can exhibit incommensurate structures, for example grain boundaries with a misorientation that brings a periodic array of atoms in one grain into contact with an array of an incommensurate periodicity in the other grain [20]. Obviously, such incommensurate structures have important consequences for the behaviors predicted for such interfaces. Technologically, superglide, superlubricity, or hypofriction – the absence of static friction –are particularly interesting properties predicted for incommensurate boundaries that could lead to many engineering applications. Although these properties have been observed for surfaces in contact in several studies on friction [21-24], experimental verification for grain boundaries of bulk materials is difficult to obtain and only one unequivocal experiment (using Au nanopillars) has been reported to date [5].

To sum up, the Cu/Nb nanolayered systems represent a platform in which gliding of one solid surface on another could be further studied. Indeed, such gliding on the interfaces between the Cu and Nb nanolayers has been predicted using molecular dynamics [7] and shown by experiments [2,3] at the grain scale. In the molecular dynamics study of Demkowicz [7] interface slip is strongly anisotropic and is suggested to be caused by the glide of misfit

dislocations which satisfy the two following criteria: (i) being able to glide in the interface plane; (ii) having a non-zero Burgers vector component in the shearing direction. To investigate the behavior of Cu/Nb interfaces in ARB nanolaminates we have developed an *in situ* shear test on a synchrotron beamline. Specially designed samples have been prepared in such a way that tensile applied force imposes shear at interfaces. X-ray diffraction has been performed during mechanical loading on BM02 beamline at ESRF (European Synchrotron Radiation Facility) in order to probe lattice strain in the sheared area. Here, we report on *in situ* mechanical tests on Cu(16 nm)/Nb(16 nm) oriented along the RD direction.

Experimental conditions

The Cu(16 nm)/Nb(16 nm) and Cu(63 nm)/Nb(63 nm) nanolaminate samples were fabricated using accumulative roll bonding (ARB) at Los Alamos National Lab, USA [25]. They have been thoroughly analyzed at IM2NP by X-ray diffraction using a four-circle X'Pert Pro MRD diffractometer from Panalytical equipped with a Cu anode (lambda = 1.54 Å). A hybrid Ge (220) monochromator was installed upstream from the sample and a parallel plate collimator was used in-between the sample and the proportional point detector, thus reducing the influence of sample misalignment. Different x-ray scattering experiments have been performed on the samples. Symmetric $\theta/2\theta$ experiments allow probing the lattice planes parallel to the sample surface. In order to investigate in detail the texture of these samples we performed pole figure measurements in the Schulz reflection geometry on various lattice plane families in Cu and in Nb.

To promote shear loading parallel to the Cu/Nb interfaces along either the rolling or the transverse directions a specific sample geometry has been prepared according to the ASTM B831-14 norm. Two notches with a width of 200 µm each are cut across the gauge. The sample geometry has been optimized by Finite Element Elastic Modelling using COMSOL Multiphysics. Here, for simplicity, the von Mises stress was calculated for a pure Cu sample with a length of 1 cm, a width of 2 mm, and a thickness of 500 µm considering the anisotropic elastic constants of Cu taken from literature. With such a geometry a shear stress of about 1 GPa is expected in the central zone for an applied tensile force of 660 N. Test samples have been prepared by electromachining out of ARB plates (Figure 1).

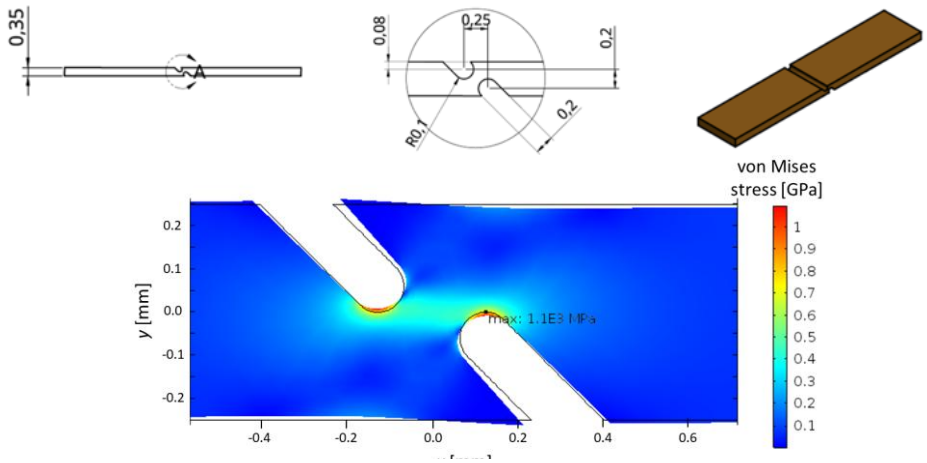

Figure 1: Typical geometry of test specimens. Notches allow the central zone to evidence shear loading when the test specimen is loaded in tension. FEM simulation of the von Mises stress in a Cu sample with two notches of 200 µm in size, an inter-notch distance of 250 µm,

and an offset of 60 µm of the two notches within the sample thickness for an applied tensile load of 660 N.

The last 15 years have witnessed a real revolution in the development of small X-ray beams. Progress in X-ray focusing optics allows nowadays scanning X-ray diffraction mapping to be performed routinely [26,27] and combined with various solicitations such as mechanical loading. In the present study notched samples have been loaded in tension using the machine "Bulky" developed at Ecole des Mines, Paris [28]. Mounting Bulky on the goniometer of BM02 beamline at ESRF in Grenoble (France) allowed for *in situ* mechanical tests. The energy of the 25x25 µm² (focused with KB mirrors) incident X-ray beam was fixed at 18 keV. The central part of the sample with an area of 800x400 µm^2 has been mapped in steps of 25 µm for two inclination angles χ of 90° and 70°. After proper calibration, 2D detector images are integrated yielding 1D diffraction patterns displaying intensity vs two theta. From such *I* vs 2θ diffractograms the diffraction peaks are fitted with a gaussian function to extract the integrated intensity, the peak position, and the peak breadth for each pixel of a map. The integrated intensity, the elastic strain and the peak width is then be plotted as a 2D map for each loading step.

In situ tensile tests were performed in displacement control mode. The displacement was increased in steps of 10 µm, resulting in about 8 N increments of the applied force. At each step, the displacement was held constant for a holding period of 60 min during which scanning X-ray diffraction maps were recorded.

Experimental results and discussion

The von Mises stress within a notched Cu test specimen computed by FEM simulations is presented in Fig. 1.d. A homogeneous stress field in between the notches is obtained for notches of 200 µm in size, an inter-notch distance of 250 µm, and an offset of 60 µm within the sample thickness. In contrast, stress concentrations are apparent at the edges of the two notches. For an applied tensile force of 660 N, the homogeneous stress in between the notches amounts to 500 MPa while the maximum of the von Mises stress reaches σ_{max} = 1.1 GPa at the notch edges.

Typical pole figures for a 16 nm/16 nm Cu/Nb sample are shown in Figure 2.

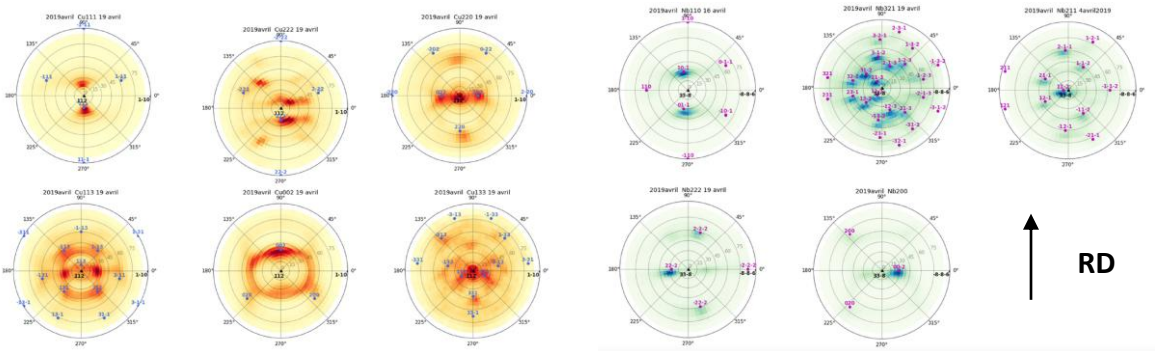

Figure 2: Pole figures for Cu (a) and Nb (b) measured on 16 nm / 16 nm ARB sample. RD is the rolling direction [reference to already published paper in Nanomaterials/MRS Advances].

These pole figures evidence a clear crystallographic anisotropy of the ARB plates, as a result of the fabrication process. In both cases sheet plane is {112}. The main observed orientation is {ND} <RD>: Cu {112} <111> Nb {112} <110> where RD, TD and ND stand for Rolling Direction, Transverse Direction, and Normal Direction, respectively. This texture, which results from the severe plastic deformation undergone by the two metals during the rolling process has already been reported in the literature [8,18]. This macroscopic mutual orientation between Cu and Nb in ARB nanolaminates translates in a distinctive Cu/Nb interface structure and has a great influence on the mechanical behavior.
From the θ/2θ scans a line profile analysis has been performed by fitting the Bragg peak profiles from Cu 111, Cu 222, Nb 110, Nb 220 using a Pseudo-Voigt function. The integral breadth deduced from these fits has been converted in reciprocal space and plotted as a function of the norm of the scattering vector ***q***. The coherent domain size L as well as the microstrain ε has been then extracted, respectively, from the intercept and the slope (Williamson-Hall plot). The corresponding results are given in Table 1.

Sample	L_{Cu} (nm)	ε_{Cu} (10^{-3})	L_{Nb} (nm)	ε_{Nb} (10^{-3})
ARB16	51	2	19	4.8
ARB63	25	1.2	18	-

Table 1: Coherent domain size (L) and microstrain (ε) in Cu and Nb sublayers extracted from line profile analysis and Williamson-Hall plot.

The larger microstrains in ARB samples with 16 nm thick nanolamellas (ARB16) as compared to sheets with 63 nm thick nanolamellas (ARB63) agree with a larger amount of plastic deformation undergone by ARB16.
Finally, residual stresses have been analysed using the $\sin^2\psi$ method on Cu 022 and Nb 112 Bragg peaks at three in-plane azimuths (0, 45 and 90°). In the two ARB samples Cu and Nb layers are under large compression (about – 450 MPa in Cu and – 620 MPa in Nb). In-plane stress is roughly isotropic in Cu but anisotropic in Nb (factor two higher stress along RD as compared to TD).

Figure 3.a and b show typical diffraction maps for sample ARB16 along RD. The integrated intensity from Cu 111 peak (Fig. 3.a) allows visualizing the notches on the sample surface and thus proper positioning of the areas of interest. In the strain map (Fig. 3.b) deduced from the gaussian fitting of the diffraction peak position only the spatial positions where diffracted intensity is non-zero make sense. In the sheared zone strains smaller than 0.1 % are detected. The high-stress zones expected at the edge of the notches visible in the FE simulation (see Fig. 1(d)), could however not be resolved due to the size of the employed X-ray probe of 25 µm while the high-stress zone extends only few micrometers.

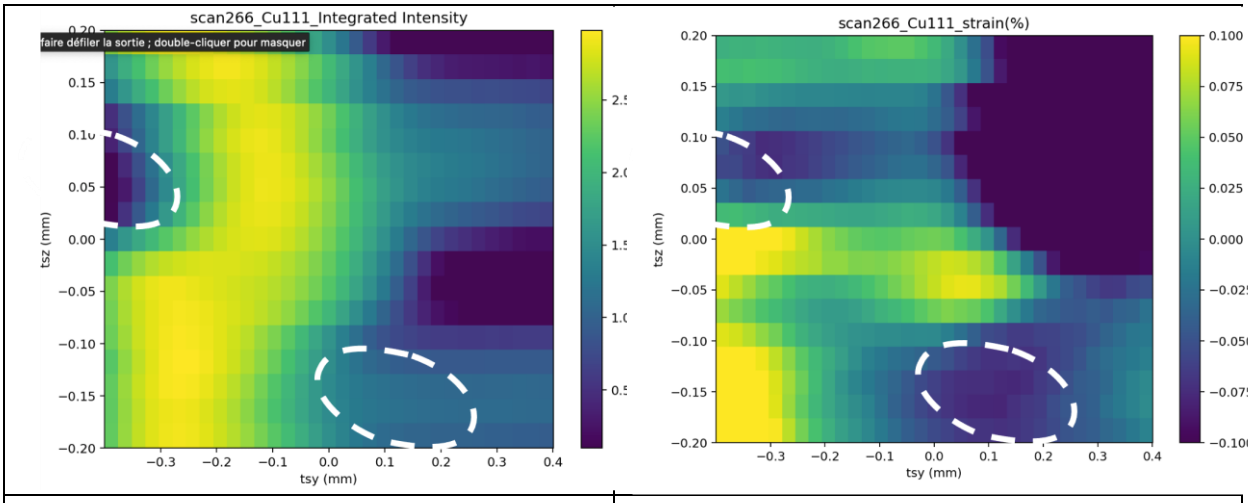

(a) (b)

Figure 3: Sample Cu(16)/Nb(16) RD. Applied load 42 N. (a) Map of Cu 111 diffracted intensity in the sheared zone. (b) Map of strain (%) in the sheared zone from Cu111. chi = 90°. Values are derived from Gaussian fitting of diffraction peak. White dotted ellipses indicate the position of the two notches.

Figure 4.a shows a typical loading curve for sample ARB16 along RD direction. The plateaus correspond to holding times at constant displacement during which the central part of the sample was mapped in diffraction. One notices some relaxation of the force during these long dwells of about one hour. The strain in the center of the sheared zone is shown for Cu in figure 4.b (sample Cu(16)/Nb(16) RD). It shows an elastic behavior of the Cu layers.

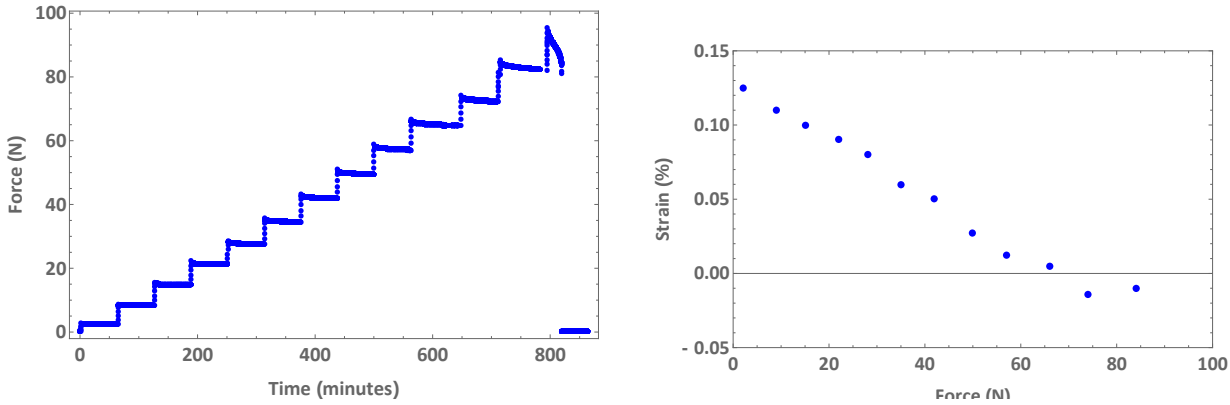

(a) (b)

Figure 3: Sample Cu(16)/Nb(16) RD. (a) Loading curve on beamline BM02 that showed brittle failure at about 80 N. (b) Strain (from X-ray diffraction) in the center of the sheared zone from Cu111. chi = 90°.

From Figure 4.a it appears that the sample broke at an applied force of about 90 N. The same behavior was observed for other samples with Cu and Nb thickness in the same range (even from other providers). This translates into a tensile stress of the order of 400 MPa, much lower than what has been reported in [1]. This early brittle failure may have been caused by crack initiation from the notch inner surfaces. A careful etching/polishing of these surfaces should be done in the future.

Conclusions

In situ shear testing of Cu/Nb ARB nanolaminates has been performed on BM02 – ESRF synchrotron beamline. Pristine samples show a strong anisotropic texture {ND} <RD>: Cu {112} <111> Nb {112} <110>. Dedicated test specimens have been prepared from the ARB plates in order to promote shear loading of interfaces upon tensile stretching. The first measurements show early brittle failure, probably caused by crack initiation from the inner surfaces of the notches.

Acknowledgments

We acknowledge co-funding provided by the ANR (Agence Nationale de la Recherche) of the French government through the Grant ANR18-CE09-003801 (Street Art Nano) and the National Research Foundation (NRF) of the Singaporean government through the Grant NRF2018-NRF-ANR042 (Street Art Nano).
We would like to thank ESRF synchrotron for allocating beamtime on BM02 beamline. Nils Blanc and Gilbert Chahine are thanked for their support during the experiment.
We thank Dr. Nathan Mara from Los Alamos National Laboratory and Prof. Irene Beyerlein from the University of California, Santa Barbara for providing Cu/Nb ARB laminates.

References

[1] T. Nizolek, I.J. Beyerlein, N.A. Mara, J.T. Avallone, T.M. Pollock, Appl. Phy. Lett., 051903 (2016).
[2] I. Radchenko *et al*., Acta Materialia, 156, 125 (2018).
[3] H.P. Anwarali, I. Radchenko, N. Li, A.S. Budiman, Materials Science and Engineering A 738, 253 (2018).
[4] J.E. Sacco, J.B. Sokoloff, Phys. Rev. B 18, 6549 (1978).
[5] F. Lancon *et al*., Nano Lett. 10, 695 (2010).
[6] J. Friedel, P.G. de Gennes, Phil. Mag. 87, 39 (2007).
[7] M.J. Demkowicz, L. Thilly, Acta Mater. 59, 7744 (2011).
[8] R. Sahay *et al*., Nanomaterials 12, 308 (2022).
[9] R. Sahay *et al*., Mater. Res. Soc. (MRS) Advances 6, 495 (2021).
[10] J. Wang *et al*., Acta Materialia 56, 3109 (2008).
[11] I.J. Beyerlein *et al*., Journal of Materials Research. 28, 1799 (2013).
[12] A. Misra, J. Hirth, R. Hoagland, Acta Materialia 53, 4817 (2005).
[13] A. Misra, R. Hoagland, H. Kung, Philosophical Magazine. 84, 1021 (2004).
[14] A. Misra, M. Demkowicz, X. Zhang, R. Hoagland, JOM. 59, 62 (2007).
[15] M. Demkowicz, Y. Wang, R. Hoagland, O. Anderoglu, Nucl. Instr. Meth. Phys. Res. B 261, 524 (2007).
[16] W. Han, E. Cerreta, N. Mara, I. Beyerlein, J. Carpenter, S. Zheng, Acta Materialia. 63, 150 (2014).
[17] J. Carpenter, S. Zheng, R. Zhang, S. Vogel, I. Beyerlein, N. Mara, Philosophical Magazine. 93, 718 (2013).
[18] I.J. Beyerlein et al., JOM 64, 1192 (2012).
[19] M. Demkowicz, Y. Wang, R. Hoagland, O. Anderoglu, Nucl. Instr. Meth. Phys. Res. B 261, 524 (2007).

[20] A. Sutton, R. Balluffi, Interfaces in Crystalline Materials; Oxford University Press: New York, 1995.
[21] J.S. Ko, A.J. Gellman, Langmuir 16, 8343 (2000).
[22] M. Dienwiebel *et al*., Phys. Rev. Lett. 92, 126101 (2004).
[23] A. Socoliuc *et al*., Phys. Rev. Lett. 92, 134401 (2004).
[24] J.Y. Park *et al*., Science 309, 1354 (2005).
[25] J. S. Carpenter *et al*., Metallurgical and Materials Transactions A 45, 2192 (2014).
[26] T. Cornelius and O. Thomas, Progress in Materials Science 94, 384 (2018).
[27] O. Thomas, S. Labat, T. Cornelius, M.I. Richard, Nanomaterials 12, 1363 (2022).
[28] M. Pelerin, A. King, L. Laiarinandrasana, H. Proudhon, Integrating Materials and Manufacturing Innovation 8, 378 (2019).